THE THERMAL EVOLUTION FOLLOWING A SUPERBURST ON AN ACCRETING NEUTRON STAR

ANDREW CUMMING[1] AND JARED MACBETH
Department of Astronomy and Astrophysics, University of California, Santa Cruz, CA 95064; cumming@ucolick.org
Draft version February 2, 2008

ABSTRACT

Superbursts are very energetic Type I X-ray bursts discovered in recent years by long term monitoring of X-ray bursters, and believed to be due to unstable ignition of carbon in the deep ocean of the neutron star. In this Letter, we follow the thermal evolution of the surface layers as they cool following the burst. The resulting light curves agree very well with observations for layer masses in the range 10^{25}–10^{26} g expected from ignition calculations, and for an energy release $\gtrsim 10^{17}$ erg per gram during the flash. We show that at late times the cooling flux from the layer decays as a power law $F \propto t^{-4/3}$, giving timescales for quenching of normal Type I bursting of weeks, in good agreement with observational limits. We show that simultaneous modelling of superburst lightcurves and quenching times promises to constrain both the thickness of the fuel layer and the energy deposited.

Subject headings: accretion, accretion disks-X-rays:bursts-stars:neutron

1. INTRODUCTION

Type I X-ray bursts from accreting neutron stars in low mass X-ray binaries involve unstable thermonuclear burning of accreted hydrogen (H) and helium (He) (Lewin, van Paradijs, & Taam 1995). In the last few years, long term monitoring of X-ray bursters by BeppoSAX and the Rossi X-Ray Timing Explorer (RXTE) has revealed a new class of very energetic Type I X-ray bursts, now known as "superbursts" (see Strohmayer & Bildsten 2003; Kuulkers 2003 for reviews). The 10^{42} erg energies and several hour durations of superbursts are 100–1000 times greater than usual Type I bursts. In addition, they are rare: so far 8 have been seen from 7 sources, with recurrence times not well-constrained, but estimated as ~ 1 year (Kuulkers 2002; in 't Zand et al. 2003; Wijnands 2001), instead of hours to days for usual Type I bursts.

The current picture is that superbursts are due to unstable ignition of carbon at densities $\rho \sim 10^8$–10^9 g cm^{-3}. Hydrogen and helium burn at $\rho \sim 10^5$–10^6 g cm^{-3} via the rp-process (Wallace & Woosley 1981), producing chiefly heavy elements beyond the iron group (including nuclei as massive as $A = 104$; Schatz et al. 2001), but with some residual carbon (mass fraction $X_C \sim 0.01$–0.1) (Schatz et al. 2003). Cumming & Bildsten (2001) (hereafter CB01) showed that this small amount of carbon can ignite unstably once the mass of the ash layer reaches $\sim 10^{25}$ g (see also Strohmayer & Brown 2002). This fits well with observed superburst energies for $X_C \approx 0.1$ and an energy release from the nuclear burning of 1 MeV per nucleon. The low thermal conductivity of the rp-process ashes gives a large temperature gradient and ignition at the required mass (CB01). The heavy nuclei may also photodisintegrate to iron group during the flash, enhancing the nuclear energy release (Schatz, Bildsten, & Cumming 2003). Therefore superbursts offer an opportunity to study the rp-process ashes.

Previous authors used one-zone models to estimate the time-dependence of the flash (CB01; Strohmayer & Brown 2002). In this paper, we present the first multi-zone models of the cooling phase of superbursts. Unlike normal Type I bursts, the time to burn the fuel is much less than the convective turnover time. We therefore assume that the fuel burns locally and instantaneously in place, without significant verti-

cal mixing. We do not calculate ignition conditions, but rather treat the amount of energy deposited and the thickness of the fuel layer as free parameters[2]. In §2, we describe our calculations of the subsequent thermal evolution of the layer, and present a simple analytic model which helps to understand the numerical results. At late times, the flux evolves as a power law in time rather than the exponential decay found by CB01 for a one-zone model. In §3, we use the long term flux evolution of the layer to predict the timescale of quenching of Type I bursts after the superburst, and compare to observations.

2. TIME EVOLUTION OF THE SUPERBURST

After the fuel burns, the cooling of the layer is described by the entropy equation

$$c_P \frac{\partial T}{\partial t} = -\epsilon_\nu - \frac{1}{\rho} \frac{\partial F}{\partial r} \qquad (1)$$

where the heat flux is $F = -K(\partial T/\partial r)$, and ϵ_ν is the neutrino energy loss rate. The layer remains in hydrostatic balance, in which case a useful independent coordinate is the column depth y into the star (units: g cm^{-2}), where $dy = -\rho dr$, giving a pressure $P = gy$. The surface gravity is $g = (GM/R^2)(1+z)$, where $1+z = (1 - 2GM/Rc^2)^{-1/2}$ is the gravitational redshift factor. In this paper, we assume $M = 1.4M_\odot$ and $R = 10$km, giving $z = 0.31$ and $g_{14} = g/10^{14}$ cm s$^{-2} = 2.45$.

To find the temperature profile just after the fuel burns, we deposit an energy $E_{nuc} = E_{17} 10^{17}$ erg g^{-1} throughout the layer. Since carbon burning to iron gives $\approx 10^{18}$ erg g^{-1}, we expect $E_{17} = 1$ to correspond to $X_C \approx 0.05$–0.1, depending on how much energy is contributed by photodisintegration (Schatz et al. 2003). At each depth, we calculate the temperature of the layer, T_f, from $\int_{T_i}^{T_f} c_P dT = E_{nuc}$, where T_i the initial temperature. Following CB01, a simple analytic estimate of T_f is as follows. The electrons are degenerate and relativistic for $\rho \gtrsim 10^7$ g cm^{-3}, giving $\rho Y_e = 1.5 \times 10^8$ g cm^{-3} $P_{26}^{3/4}$, Fermi energy $E_F = 2.7$ MeV $P_{26}^{1/4}$, and pressure scale height

---

[1] Hubble Fellow

[2] This is a similar approach to Eichler & Cheng (1989) who studied the thermal response of a neutron star to energy deposition at different depths. However, the transient events they consider are less energetic than superbursts.
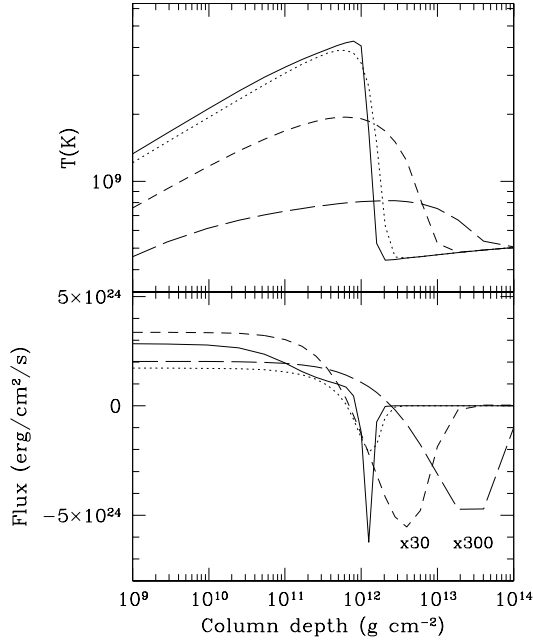
FIG. 1.— Temperature and flux profiles for $y_b = 10^{12}$ g cm^{-2}, $E_{17} = 1$, and $t = 10$ minutes (solid lines), 1 hour (dotted lines), 1 day (short-dashed lines), and 10 days (long-dashed lines) after ignition. In the lower panel, the $t = 1$ hour (1 day) flux profile is shown scaled by a factor of 30 (300).
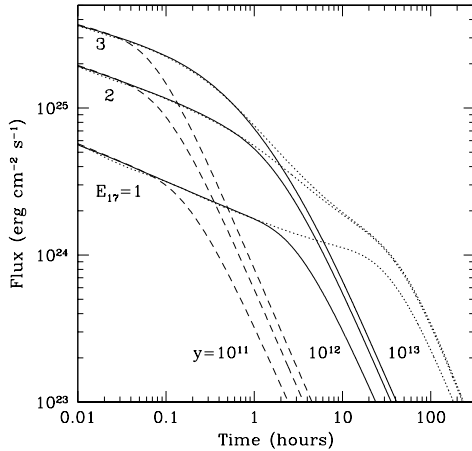

FIG. 2.— Flux from the surface against time for different values for the energy release E_{17} and layer thickness y_b (in g cm^{-2}).
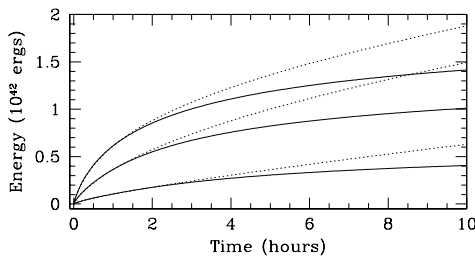

FIG. 3.— Cumulative energy released from the surface as a function of time, for $y_b = 10^{12}$ (solid lines) and 10^{13} g cm^{-2} (dotted lines) and in each case (bottom to top) $E_{17} = 1$, 2, and 3.

$H = y/\rho = 67$ m $P_{26}^{1/4} Y_e/g_{14}$, where $P = P_{26} 10^{26}$ erg cm^{-3}. The heat capacity c_P is determined mainly by the electrons, $c_P \approx \pi^2(Y_e k_B/m_p)(k_B T/E_F) = 2.6 \times 10^7$ erg g^{-1} K^{-1} $T_9 Y_e P_{26}^{-1/4}$. Integrating and assuming $T_i \ll T_f$, we find the convectively stable temperature profile $T_f = 3.6 \times 10^9$ K $E_{17}^{1/2} P_{26}^{1/8} Y_e^{-1/8}$, insensitive to depth and depending mainly on E_{17}.

Our thermal evolution code uses the method of lines, in which the right hand side of equation (1) is differenced over a spatial grid, and the resulting set of ordinary differential equations integrated using a stiff integrator. We choose a uniform grid in $\sinh^{-1}(\log y/y_b)$, which concentrates grid points around the base of the layer y_b, resolving the initial temperature discontinuity. We place the outer boundary at $y = 10^8$ g cm^{-2}, and set flux $\propto T^4$ there; at the inner boundary, typically $y \approx 10^{14}$ g cm^{-2}, we assume vanishing flux. We assume the layer is heated before the flash by a 10^{21} erg cm^{-2} s^{-1} flux from the crust, and that all the fuel burns to ^{56}Fe. Our results are not sensitive to the details of the grid, or boundary conditions (for times longer than the thermal time at the top zone). We calculate the equation of state, opacity, neutrino emissivity, and heat capacity as described by Schatz et al. (2003).

Figure 1 shows temperature and flux profiles 10 minutes, 1 hour, 1 day, and 10 days after ignition for a model with $E_{17} = 1$ and $y_b = 10^{12}$ g cm^{-2}. Figure 2 shows a series of lightcurves for different y_b and E_{17}. At early times, as the outer parts of the layer thermally adjust, the radiative flux depends mostly on E_{17}. At late times, after the cooling wave reaches the base of the layer, the flux depends mostly on y_b, and falls off as a power law $F \propto t^{-4/3}$. Figure 3 shows the cumulative energy release for $y_b = 10^{12}$ and 10^{13} g cm^{-2} and $E_{17} = 1$–3. In the first few hours, the energy released from the surface is $\approx 10^{42}$ ergs, the exact value being mainly sensitive to E_{17}, rather than depth. A significant fraction of the heat is initially conducted inwards and released on a longer timescale, as pointed out by Strohmayer & Brown (2002).

The physical reason for the late-time power law flux decay is that as time evolves, the peak of the temperature profile moves to greater depths where the thermal timescale to the surface is longer[3] (see Fig. 1). The simplest analytic model is a slab with constant thermal diffusivity D, whose temperature is perturbed close to the surface, for example at a depth $x = a$ (where $x = 0$ is the surface). For a delta-function perturbation initially, the temperature evolution is given by the Green's function[4]

$$T(x,t) = \frac{1}{\sqrt{\pi D t}} \sinh\left(\frac{ax}{2Dt}\right) \exp\left(-\frac{x^2 + a^2}{4Dt}\right) \qquad (2)$$

and the surface flux is $F \propto (\partial T/\partial x)_{x=0} \propto t^{-3/2} \exp(-\tau/t)$, where τ is the thermal time at the initial heating depth $\tau = 4a^2/D$. For an initial "top hat" temperature profile $T(x < a) = 1$, $T(x > a) = 0$, the surface flux is $F \propto (\tau/t)^{1/2}\left[1 - \exp(-\tau/t)\right]$. For $t < \tau$, before the cooling wave reaches the base of the layer, $F \propto t^{-1/2}$; for $t > \tau$, the solution

[3] A similar problem is ohmic decay of crustal magnetic fields, where power law decay is also expected (Sang & Chanmugam 1987; Urpin, Chanmugam, & Sang 1994)

[4] A simple way to obtain this result is to apply the method of images to the Green's function for an unbounded domain $T(x,t) \propto t^{-1/2} \exp\left(-x^2/4Dt\right)$. Eichler & Cheng (1989) derive a similar result for a power law dependence of conductivity on depth, which also shows self-similar behavior at late times (see Lyubarsky, Eichler, & Thompson 2002 for a recent application to cooling of SGR 1900+14 after an outburst).

is independent of the initial temperature profile, and $F \propto t^{-3/2}$.

The numerical results show a similar behavior, although with different power law indices. The relevant timescale in this case is $t_{\rm cool} = H^2/D$, where $D = K/\rho c_P$. The electron conductivity is $K = \pi^2 n_e k_B^2 T/3 m_\star \nu_c$, where $m_\star = E_F/c^2$, and ν_c is the electron collision frequency. When electrons dominate the heat capacity, the thermal diffusivity takes the particularly simple temperature-independent form $D = c^2/3\nu_c$. For electron-ion collisions, $\nu_c = 9.3 \times 10^{16}$ s^{-1} $P_{26}^{1/4} \langle Z^2/A \rangle \Lambda_{ei}/Y_e$ (e.g. see Appendix of Schatz et al. 1999), giving

$$t_{\rm cool} = 3.8 \text{ hrs } y_{12}^{3/4} \left(\frac{Y_e \langle Z^2/A \rangle \Lambda_{ei}}{6} \right) \left(\frac{g_{14}}{2.45} \right)^{-5/4} \quad (3)$$

(see also eq. [10] of CB01), where we insert the appropriate numbers for ^{56}Fe composition. The simple "top hat" solution for constant conductivity motivates a fit to the numerical solutions,

$$F_{25} = 0.2 \, t_{\rm hr}^{-0.2} \, E_{17}^{7/4} \left[1 - \exp\left(-0.63 \, t_{\rm cool}^{4/3} E_{17}^{-5/4} t_{\rm hr}^{-1.13} \right) \right], \quad (4)$$

where $t_{\rm hr} = t/1$ hour. For $t > t_{\rm cool}$, $F_{25} = 0.13 \, E_{17}^{1/2} (t/t_{\rm cool})^{-4/3}$. The transition from $F \propto t^{-0.2}$ to $F \propto t^{-4/3}$ occurs when $t/t_{\rm cool} \approx E_{17}^{-1.1}$.

Equation (4) fits the numerical results to better than a factor of two for models without substantial neutrino emission. As emphasised by Strohmayer & Brown (2002), neutrino cooling is important for large carbon fractions: it depresses the flux at $t \approx 5$–10 hours for the models with $E_{17} = 2$ and 3, $y = 10^{13}$ g cm^{-2} in Figure 2. Whenever neutrinos dominate the cooling, the peak temperature is large enough that emission is by pair annhilation. A good fit to the neutrino energy loss rate is $\epsilon_\nu \approx 10^4$ erg g^{-1} s$^{-1} T_9^{12} y_{12}^{-3/2}$, giving a cooling time $t_\nu = c_P T/\epsilon_\nu = 2.5 \times 10^{12}$ s $y_{12}^{5/4} T_9^{-10}$. Inserting the peak temperature from equation (2) gives $t_\nu \approx 300$ hrs E_{17}^{-5}. Neutrinos dominate when $t_\nu < t_{\rm cool}$, or when $E_{17} > 2.3 \, y_{12}^{-3/20}$.

3. COMPARISON TO OBSERVATIONS

The cooling curves in Figure 2 compare well with observed lightcurves, including a rapid initial decay on hour timescales, followed by an extended tail of emission (as observed following some superbursts, e.g. KS 1731-260, Kuulkers et al. 2002; Ser X-1, Cornelisse et al. 2002). We will present a detailed comparison with the observed superburst lightcurves in a future paper. The initial decay from the peak depends mostly on E_{17}, and so it should be possible to constrain the amount of fuel consumed in the superburst. Our models do not resolve the peak itself, since this depends on the details of how the burning propagates out to the surface; however, for $E_{17} \gtrsim 2$–3, the flux exceeds the Eddington flux, $F_{\rm Edd} = 3 \times 10^{25}$ erg cm^{-2} s$^{-1}/(1+X)$, where X is the H fraction, for timescales of minutes. Superburst peak luminosities are generally less than the Eddington luminosity (Kuulkers 2003), implying $E_{17} \lesssim 2$. The one exception is the superburst from 4U 1820-30, which showed dramatic photospheric radius expansion lasting for several minutes (Strohmayer & Brown 2002). This is consistent with the proposal that this source, which accretes and burns He rich material, produces large quantities of carbon (Strohmayer & Brown 2002; Cumming 2003a). The transition to the late-time power law occurs after $t \approx 4$ h $E_{17}^{-1.11} y_{12}^{3/4}$ (eq. [5]), which corresponds to $F_{25} \approx 0.13 E_{17}^2$. It may therefore be possible to measure the
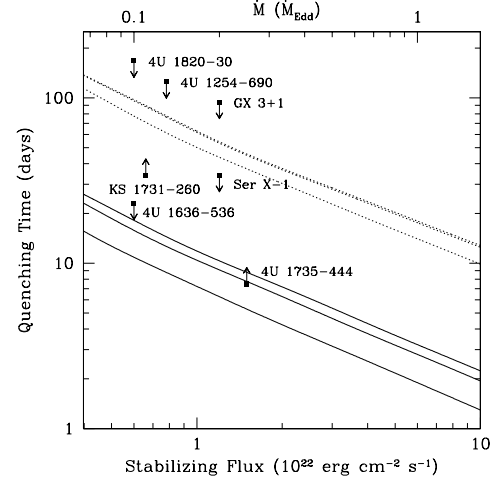

FIG. 4.— Observed and predicted quenching timescales of normal Type I bursts following a superburst. We show the predicted quenching time for $y_b = 10^{12}$ (solid lines) and 10^{13} g cm^{-2} (dotted lines) as a function of both the critical flux needed to stabilize H/He burning $F_{\rm crit}$, and the accretion rate (given in terms of $F_{\rm crit}$ by eq. [5]). For each value of y_b, we show curves for (bottom to top) $E_{17} = 1$, 2 and 3. The observed upper or lower limits on $t_{\rm quench}$, and the estimated $\dot{M}$, are taken from Table 1 of Kuulkers 2003, with an updated value for 4U 1636-53 (Kuulkers, private communication).

power law decay using superburst tails, although this depends upon being able to subtract out the underlying accretion luminosity, $F_{\rm accr,25} \approx 0.1 \, (\dot{M}/0.1\dot{M}_{\rm Edd})$, in a reliable way.

Another way to probe the late-time cooling is to use the remarkable observation that Type I bursts disappear (are "quenched") for $t_{\rm quench} \approx$ weeks following the superburst (e.g. Kuulkers 2003). CB01 proposed that the cooling flux from the superburst temporarily stabilizes the H/He burning. An estimate of the critical stabilizing flux, $F_{\rm crit}$, is as follows. The condition for temperature fluctuations to grow, and unstable He ignition to occur, is $\nu \epsilon_{3\alpha} = \eta \epsilon_{\rm cool}$ (Fushiki & Lamb 1987), where $\epsilon_{3\alpha}$ is the triple alpha (3α) energy production rate, $\epsilon_{\rm cool}$ is a local approximation to the cooling rate, and ν and η are the respective temperature sensitivities. For a large flux from below, the He burns stably before reaching this ignition condition, at a depth where the time to accumulate the layer equals the He burning time, $y/\dot{m} = Y Q_{3\alpha}/\epsilon_{3\alpha}$, where Y is the He mass fraction, $\dot{m}$ is the local accretion rate per unit area, and $Q_{3\alpha} = 5.84 \times 10^{17}$ erg g$^{-1} = 0.606$ MeV per nucleon is the 3α energy release. At the transition from unstable to stable burning, both criteria are satisfied at the base of the H/He layer. Using the first condition to eliminate $\epsilon_{3\alpha}$ from the second, and writing $\epsilon_{\rm cool} \approx F/y$, gives $F = \nu \dot{m} Q_{3\alpha} Y/\eta = 6.2 \times 10^{22}$ erg cm^{-2} s$^{-1} (\dot{m}/\dot{m}_{\rm Edd})(Y/0.3)(\nu/4\eta)$. Some of this flux is provided by hot CNO burning of accreted H, $F_H \approx \epsilon_H y = 5.8 \times 10^{21}$ erg cm^{-2} s$^{-1} y_8 (Z/0.01)$ (Cumming & Bildsten 2000; Z is the metallicity); the remainder is $F_{\rm crit} = F - F_H$. This estimate agrees well with a more detailed calculation using the ignition models of Cumming & Bildsten (2000), in which we find $F_{\rm crit} \approx \dot{m} Q_{3\alpha} \approx 0.7$ MeV per accreted nucleon, almost independent of $\dot{M}$. Therefore,

$$F_{\rm crit,22} \approx 6 \, (\dot{m}/\dot{m}_{\rm Edd}) \quad (5)$$

(see also Paczynski 1983a; Bildsten 1995). Equation (5) in

the limit $t \gg t_{\rm cool}$ gives

$$t_{\rm quench} = 38\, t_{\rm cool}\, F_{\rm crit,22}^{-3/4} E_{17}^{3/8} = 6\,{\rm days}\; y_{12}^{3/4} F_{\rm crit,22}^{-3/4} E_{17}^{3/8}, \qquad (6)$$

which gives $t_{\rm quench}$ in terms of the thickness of the layer and energy release.

Figure 5 compares the predicted and observed quenching times. The observations of $t_{\rm quench}$ and accretion rates (used to find $F_{\rm crit}$ from eq. [5]) are taken from Kuulkers (2003) (except for 4U 1636-53, which has a revised upper limit of 23 days, Kuulkers private communication). The observations are upper or lower limits only: nonetheless, the general agreement is very good and supports the quenching picture suggested by CB01. There is much to learn from a careful comparison of superburst lightcurves and the corresponding quenching times, separately constraining both E_{17} and y_b.

4. SUMMARY AND CONCLUSIONS

We have presented the first multi-zone models of the cooling phase of superbursts. The flux decay is not exponential, but power-law (eq. [5]). For $t < t_{\rm cool}$, where $t_{\rm cool}$ is the cooling time at the base of the layer, the flux depends mostly on the energy release E_{17}, and is insensitive to depth: the inwards travelling cooling wave does not yet know that the layer has a finite thickness. For $t > t_{\rm cool}$, the flux decays as a power law $F \propto t^{-4/3}$, independent of the initial temperature profile. The power law decay at late times gives predicted Type I burst quenching times of weeks (eq. [6]), consistent with observational limits. Future comparisons of both superburst lightcurves and quenching times with observations will constrain both the thickness of the fuel layer and the energy deposited, particularly when combined with models of normal Type I bursts from the same source (Cumming 2003a,b).

There is still much to be done in terms of theory. Perhaps the most important issues are the physics of the rise (which sets the initial condition for our simulations), and production of the fuel. Important clues to the first are the observed precursors to superbursts, which may be normal Type I bursts ignited by the superburst. Recent progress has been made on the second, with indications from both theory (Schatz et al. 2003; Woosley et al. 2003) and observations (in 't Zand et al. 2003) that stable burning may be required to produce enough carbon to power superbursts. A self-consistent model of H/He burning, followed by accumulation and ignition of the ashes may require a better understanding of the transition from unstable to stable burning observed in normal Type I bursting (e.g. Cornelisse et al. 2003).

REFERENCES

Bildsten, L. 1995, ApJ, 438, 852
Brown, E. F., & Bildsten, L. 1998, ApJ, 496, 915
Cornelisse, R., Kuulkers, E., in't Zand, J. J. M., Verbunt, F., & Heise, J. 2002, A&A, 382, 174
Cornelisse, R. et al. 2003, A&A, 405, 1033
Cumming, A. 2003a, ApJ, 595, 1077
Cumming, A. 2003b, in "The Restless High-Energy Universe" (Amsterdam, May 5-8, 2003), ed. E.P.J. van den Heuvel, J.J.M. in 't Zand, and R.A.M.J. Wijers (astro-ph/0309626)
Cumming, A., & Bildsten, L. 2001, ApJ, 559, L127 (CB01)
Eichler, D., & Cheng, A. F. 1989, ApJ, 336, 360
Fushiki, I., & Lamb, D. Q. 1987, ApJ, 323, L55
in't Zand, J. J. M., Kuulkers, E., Verbunt, F., Heise, J., & Cornelisse, R. 2003, A&A, 411, L487
Itoh, N., Hayashi, H., Nishikawa, A., & Kohyama, Y. 1996, ApJS, 102, 411
Kuulkers, E., 2002, A&A, 383, L5
Kuulkers, E., 2003, in "The Restless High-Energy Universe" (Amsterdam, May 5-8, 2003), ed. E.P.J. van den Heuvel, J.J.M. in 't Zand, and R.A.M.J. Wijers (astro-ph/0310402)
Kuulkers, E. et al. 2002, A&A, 382, 503
Lewin, W. H. G., van Paradijs, J., & Taam, R. E. 1995, in X-Ray Binaries, ed. W. H. G. Lewin, J. van Paradijs, & E. P. J. van den Heuvel (Cambridge: CUP), 175

Lyubarsky, Y., Eichler, D., & Thompson, C. 2002, ApJ, 580, L69
Paczynski, B., 1983, ApJ, 264, 282
Paczynski, B., 1983, ApJ, 267, 315
Potekhin, A. Y. & Chabrier, G. 2000, Phys. Rev. E, 62, 8554
Sang, Y. & Chanmugam, G. 1987, ApJ, 323, L61
Schatz, H., et al. 2001, Phys. Rev. Lett., 86, 3471
Schatz, H., Bildsten, L., & Cumming, A. 2003, ApJ, 583, L87
Schatz, H., Bildsten, L., Cumming, A., & Wiescher, M. 1999, ApJ, 524, 1014
Schatz, H., Bildsten, L., Cumming, A., & Ouellette, M. 2003, Nucl. Phys. A, 718, 247
Strohmayer, T. E., & Bildsten, L. 2003, in Compact Stellar X-Ray Sources, eds. W.H.G. Lewin and M. van der Klis (Cambridge: Cambridge University Press) (astro-ph/0301544)
Strohmayer, T. E., & Brown, E. F., 2002, ApJ, 566, 1045
Urpin, V. A., Chanmugam, G., & Sang, Y. 1994, ApJ, 433, 780
Wallace, R. K. & Woosley, S. E. 1981, ApJS, 45, 389
Wijnands, R. 2001, ApJ, 554, L59
Woosley, S. E. et al. 2003, ApJS, in press (astro-ph/0307425)